Search for $\gamma\gamma$ decays of a Higgs boson produced in association with a fermion pair in e^+e^- collisions at LEP

R. Barate, D. Decamp, P. Ghez, C. Goy, S. Jezequel, J P. Lees, F. Martin, E. Merle, M N. Minard, B. Pietrzyk, et al.

EUROPEAN ORGANIZATION FOR NUCLEAR RESEARCH (CERN)

CERN-EP/2000-083
June 29, 2000

Search for $\gamma\gamma$ decays of a Higgs boson produced in association with a fermion pair in e^+e^- collisions at LEP

The ALEPH Collaboration[1])

Abstract

A search for $\gamma\gamma$ decays of a Higgs boson is performed in the data sample collected at LEP with the ALEPH detector between 1991 and 1999. This corresponds to an integrated luminosity of 672 pb^{-1} at centre-of-mass energies ranging from 88 to 202 GeV. The search is based on topologies arising from a Higgs boson produced in association with a fermion pair via the Higgs-strahlung process $e^+e^- \to Hf\bar{f}$, with $f\bar{f} = \nu\bar{\nu}$, $e^+e^-, \mu^+\mu^-, \tau^+\tau^-$ or $q\bar{q}$. Twenty-two events are selected in the data, while 28 events are expected from standard model processes. An upper limit is derived, as a function of the Higgs boson mass, on the product of the $e^+e^- \to Hf\bar{f}$ cross section and the $H \to \gamma\gamma$ branching fraction. In particular, a fermiophobic Higgs boson produced with the standard model cross section is excluded at 95% confidence level for all masses below $100.7\,\mathrm{GeV}/c^2$.

(To be submitted to Physics Letters B)

[1])See next pages for the list of authors

R. Barate, D. Decamp, P. Ghez, C. Goy, S. Jezequel, J.-P. Lees, F. Martin, E. Merle, M.-N. Minard, B. Pietrzyk

Laboratoire de Physique des Particules (LAPP), IN^{2}P^3-CNRS, F-74019 Annecy-le-Vieux Cedex, France

S. Bravo, M.P. Casado, M. Chmeissani, J.M. Crespo, E. Fernandez, M. Fernandez-Bosman, Ll. Garrido,[15] E. Graugés, J. Lopez, M. Martinez, G. Merino, R. Miquel, Ll.M. Mir, A. Pacheco, D. Paneque, H. Ruiz

Institut de Física d'Altes Energies, Universitat Autònoma de Barcelona, E-08193 Bellaterra (Barcelona), Spain[7]

A. Colaleo, D. Creanza, N. De Filippis, M. de Palma, G. Iaselli, G. Maggi, M. Maggi, S. Nuzzo, A. Ranieri, G. Raso, F. Ruggieri, G. Selvaggi, L. Silvestris, P. Tempesta, A. Tricomi,[3] G. Zito

Dipartimento di Fisica, INFN Sezione di Bari, I-70126 Bari, Italy

X. Huang, J. Lin, Q. Ouyang, T. Wang, Y. Xie, R. Xu, S. Xue, J. Zhang, L. Zhang, W. Zhao

Institute of High Energy Physics, Academia Sinica, Beijing, The People's Republic of China[8]

D. Abbaneo, G. Boix,[6] O. Buchmüller, M. Cattaneo, F. Cerutti, G. Dissertori, H. Drevermann, R.W. Forty, M. Frank, F. Gianotti, T.C. Greening, A.W. Halley, J.B. Hansen, J. Harvey, P. Janot, B. Jost, M. Kado, V. Lemaitre, P. Maley, P. Mato, A. Minten, A. Moutoussi, F. Ranjard, L. Rolandi, D. Schlatter, M. Schmitt,[20] O. Schneider,[2] P. Spagnolo, W. Tejessy, F. Teubert, E. Tournefier, A. Valassi, J.J. Ward, A.E. Wright

European Laboratory for Particle Physics (CERN), CH-1211 Geneva 23, Switzerland

Z. Ajaltouni, F. Badaud, G. Chazelle, O. Deschamps, S. Dessagne, A. Falvard, P. Gay, C. Guicheney, P. Henrard, J. Jousset, B. Michel, S. Monteil, J-C. Montret, D. Pallin, J.M. Pascolo, P. Perret, F. Podlyski

Laboratoire de Physique Corpusculaire, Université Blaise Pascal, IN^{2}P^3-CNRS, Clermont-Ferrand, F-63177 Aubière, France

J.D. Hansen, J.R. Hansen, P.H. Hansen,[1] B.S. Nilsson, A. Wäänänen

Niels Bohr Institute, 2100 Copenhagen, DK-Denmark[9]

G. Daskalakis, A. Kyriakis, C. Markou, E. Simopoulou, A. Vayaki

Nuclear Research Center Demokritos (NRCD), GR-15310 Attiki, Greece

A. Blondel,[12] J.-C. Brient, F. Machefert, A. Rougé, M. Swynghedauw, R. Tanaka H. Videau

Laboratoire de Physique Nucléaire et des Hautes Energies, Ecole Polytechnique, IN^{2}P^3-CNRS, F-91128 Palaiseau Cedex, France

E. Focardi, G. Parrini, K. Zachariadou

Dipartimento di Fisica, Università di Firenze, INFN Sezione di Firenze, I-50125 Firenze, Italy

A. Antonelli, M. Antonelli, G. Bencivenni, G. Bologna,[4] F. Bossi, P. Campana, G. Capon, V. Chiarella, P. Laurelli, G. Mannocchi,[5] F. Murtas, G.P. Murtas, L. Passalacqua, M. Pepe-Altarelli

Laboratori Nazionali dell'INFN (LNF-INFN), I-00044 Frascati, Italy

M. Chalmers, J. Kennedy, J.G. Lynch, P. Negus, V. O'Shea, B. Raeven, D. Smith, P. Teixeira-Dias, A.S. Thompson

Department of Physics and Astronomy, University of Glasgow, Glasgow G12 8QQ,United Kingdom[10]

R. Cavanaugh, S. Dhamotharan, C. Geweniger,[1] P. Hanke, V. Hepp, E.E. Kluge, G. Leibenguth, A. Putzer, K. Tittel, S. Werner,[19] M. Wunsch[19]

Kirchhoff-Institut für Physik, Universität Heidelberg, D-69120 Heidelberg, Germany[16]

H. Przysiezniak,[1] J.K. Sedgbeer, J.C. Thompson,[11] E. Thomson,[23] R. White

Department of Physics, Imperial College, London SW7 2BZ, United Kingdom[10]

V.M. Ghete, P. Girtler, E. Kneringer, D. Kuhn, G. Rudolph

Institut für Experimentalphysik, Universität Innsbruck, A-6020 Innsbruck, Austria[18]

C.K. Bowdery, P.G. Buck, D.P. Clarke, G. Ellis, A.J. Finch, F. Foster, G. Hughes, R.W.L. Jones, N.A. Robertson, M. Smizanska

Department of Physics, University of Lancaster, Lancaster LA1 4YB, United Kingdom[10]

I. Giehl, F. Hölldorfer, K. Jakobs, K. Kleinknecht, M. Kröcker, A.-S. Müller, H.-A. Nürnberger, G. Quast,[1] B. Renk, E. Rohne, H.-G. Sander, S. Schmeling, H. Wachsmuth, C. Zeitnitz, T. Ziegler

Institut für Physik, Universität Mainz, D-55099 Mainz, Germany[16]

A. Bonissent, J. Carr, P. Coyle, C. Curtil, A. Ealet, D. Fouchez, O. Leroy, T. Kachelhoffer, P. Payre, D. Rousseau, A. Tilquin

Centre de Physique des Particules de Marseille, Univ Méditerranée, IN^2*P*^{3}*-CNRS, F-13288 Marseille, France*

M. Aleppo, S. Gilardoni, F. Ragusa

Dipartimento di Fisica, Università di Milano e INFN Sezione di Milano, I-20133 Milano, Italy.

H. Dietl, G. Ganis, A. Heister, K. Hüttmann, G. Lütjens, C. Mannert, W. Männer, H.-G. Moser, S. Schael, R. Settles,[1] H. Stenzel, W. Wiedenmann, G. Wolf

Max-Planck-Institut für Physik, Werner-Heisenberg-Institut, D-80805 München, Germany[16]

P. Azzurri, J. Boucrot,[1] O. Callot, M. Davier, L. Duflot, J.-F. Grivaz, Ph. Heusse, A. Jacholkowska,[1] L. Serin, J.-J. Veillet, I. Videau,[1] J.-B. de Vivie de Régie, D. Zerwas

Laboratoire de l'Accélérateur Linéaire, Université de Paris-Sud, IN^2*P*^{3}*-CNRS, F-91898 Orsay Cedex, France*

G. Bagliesi, T. Boccali, G. Calderini, V. Ciulli, L. Foà, A. Giammanco, A. Giassi, F. Ligabue, A. Messineo, F. Palla,[1] G. Rizzo, G. Sanguinetti, A. Sciabà, G. Sguazzoni, R. Tenchini,[1] A. Venturi, P.G. Verdini

Dipartimento di Fisica dell'Università, INFN Sezione di Pisa, e Scuola Normale Superiore, I-56010 Pisa, Italy

G.A. Blair, J. Coles, G. Cowan, M.G. Green, D.E. Hutchcroft, L.T. Jones, T. Medcalf, J.A. Strong, J.H. von Wimmersperg-Toeller

Department of Physics, Royal Holloway & Bedford New College, University of London, Surrey TW20 OEX, United Kingdom[10]

R.W. Clifft, T.R. Edgecock, P.R. Norton, I.R. Tomalin

Particle Physics Dept., Rutherford Appleton Laboratory, Chilton, Didcot, Oxon OX11 OQX, United Kingdom[10]

B. Bloch-Devaux, D. Boumediene, P. Colas, B. Fabbro, G. Faïf, E. Lançon, M.-C. Lemaire, E. Locci, P. Perez, J. Rander, J.-F. Renardy, A. Rosowsky, P. Seager,[13] A. Trabelsi,[21] B. Tuchming, B. Vallage

CEA, DAPNIA/Service de Physique des Particules, CE-Saclay, F-91191 Gif-sur-Yvette Cedex, France[17]

S.N. Black, J.H. Dann, C. Loomis, H.Y. Kim, N. Konstantinidis, A.M. Litke, M.A. McNeil, G. Taylor

Institute for Particle Physics, University of California at Santa Cruz, Santa Cruz, CA 95064, USA[22]

C.N. Booth, S. Cartwright, F. Combley, P.N. Hodgson, M. Lehto, L.F. Thompson

Department of Physics, University of Sheffield, Sheffield S3 7RH, United Kingdom[10]

K. Affholderbach, A. Böhrer, S. Brandt, C. Grupen,[1] J. Hess, A. Misiejuk, G. Prange, U. Sieler

Fachbereich Physik, Universität Siegen, D-57068 Siegen, Germany[16]

C. Borean, G. Giannini, B. Gobbo

Dipartimento di Fisica, Università di Trieste e INFN Sezione di Trieste, I-34127 Trieste, Italy

H. He, J. Putz, J. Rothberg, S. Wasserbaech

Experimental Elementary Particle Physics, University of Washington, Seattle, WA 98195 U.S.A.

S.R. Armstrong, K. Cranmer, P. Elmer, D.P.S. Ferguson, Y. Gao, S. González, O.J. Hayes, H. Hu, S. Jin, J. Kile, P.A. McNamara III, J. Nielsen, W. Orejudos, Y.B. Pan, Y. Saadi, I.J. Scott, J. Walsh, J. Wu, Sau Lan Wu, X. Wu, G. Zobernig

Department of Physics, University of Wisconsin, Madison, WI 53706, USA[11]

[1]Also at CERN, 1211 Geneva 23, Switzerland.
[2]Now at Université de Lausanne, 1015 Lausanne, Switzerland.
[3]Also at Dipartimento di Fisica di Catania and INFN Sezione di Catania, 95129 Catania, Italy.
[4]Also Istituto di Fisica Generale, Università di Torino, 10125 Torino, Italy.
[5]Also Istituto di Cosmo-Geofisica del C.N.R., Torino, Italy.
[6]Supported by the Commission of the European Communities, contract ERBFMBICT982894.
[7]Supported by CICYT, Spain.
[8]Supported by the National Science Foundation of China.
[9]Supported by the Danish Natural Science Research Council.
[10]Supported by the UK Particle Physics and Astronomy Research Council.
[11]Supported by the US Department of Energy, grant DE-FG0295-ER40896.
[12]Now at Departement de Physique Corpusculaire, Université de Genève, 1211 Genève 4, Switzerland.
[13]Supported by the Commission of the European Communities, contract ERBFMBICT982874.
[14]Also at Rutherford Appleton Laboratory, Chilton, Didcot, UK.
[15]Permanent address: Universitat de Barcelona, 08208 Barcelona, Spain.
[16]Supported by the Bundesministerium für Bildung, Wissenschaft, Forschung und Technologie, Germany.
[17]Supported by the Direction des Sciences de la Matière, C.E.A.
[18]Supported by the Austrian Ministry for Science and Transport.
[19]Now at SAP AG, 69185 Walldorf, Germany
[20]Now at Harvard University, Cambridge, MA 02138, U.S.A.
[21]Now at Département de Physique, Faculté des Sciences de Tunis, 1060 Le Belvédère, Tunisia.
[22]Supported by the US Department of Energy, grant DE-FG03-92ER40689.
[23]Now at Department of Physics, Ohio State University, Columbus, OH 43210-1106, U.S.A.

1 Introduction

In general, neutral Higgs bosons do not couple directly to massless photons. For instance the standard model Higgs boson couples to photons only through loops of charged particles, *i.e.,* W's, quarks and leptons, and the branching ratio into $\gamma\gamma$ is small ($\approx 10^{-3}$ [1] for $m_H \sim 90\,GeV/c^2$). However the $\gamma\gamma$ branching fraction of Higgs bosons can be increased with respect to the standard model prediction in each of the following four configurations.

- The direct couplings to fermions are suppressed, as is the case for models with at least two Higgs multiplets [2], of which one couples only to fermions and the others only to gauge bosons. The physical states with couplings only to gauge bosons are called *fermiophobic* Higgs bosons.
- The direct couplings to gauge bosons are enhanced with anomalous couplings [3]. These couplings are described in the most general formulation with four effective six-dimensional operators with strength f_i/Λ^2, where Λ is the scale of the new underlying interaction.
- Couplings to both fermions and bosons are modified, as is the case in the minimal supersymmetric extension of the standard model (MSSM).
- Additional light, charged particles enter the loops that couple Higgs bosons and photons, as is again the case in the MSSM (charginos, squarks, sleptons, charged Higgs bosons).

With some particular choices of parameters, the branching ratio into $\gamma\gamma$ may be enhanced in the MSSM, and can reach a value close to 100% in models with fermiophobia or with anomalous gauge couplings. It is therefore possible that a Higgs boson has escaped the standard search for the Higgs-strahlung process $e^+e^- \to Hf\bar{f}$ with $H \to b\bar{b}$ [4]. In this letter, a complementary search for the Higgs-strahlung process with $H \to \gamma\gamma$ is described.

The analysis addresses all topologies arising from the $e^+e^- \to HZ^{(*)}$ process, as characterized by the charged track multiplicity of the final state: *(i)* acoplanar photons with missing energy and no charged particles for $H\nu\bar{\nu}$; *(ii)* photon pairs with exactly two charged particles identified as leptons for $H\ell^+\ell^-$; *(iii)* photon pairs accompanied with two thin, low multiplicity jets for $H\tau^+\tau^-$, from two to four charged particles; and *(iv)* photon pairs with a hadronic system for $Hq\bar{q}$ with at least five charged particles.

The analysis is performed with the data collected with the ALEPH detector from 1991 to 1999 including the Z peak data collected during the LEP 2 period. This sample corresponds to an integrated luminosity of $672\,pb^{-1}$ at centre-of-mass energies ranging from 88 to 202 GeV. Details are given in Table 1.

After a short description of the detector properties relevant for this search, the common preselection based on photon identification is reviewed in Section 3. The global search strategy is developed in Section 4. The systematic uncertainties affecting the selection efficiency are discussed in Section 5 and the results are given in Section 6.

Table 1: Integrated luminosity for the Z peak data (88-94 GeV) and high energy data (130-202 GeV). The energies are rounded to the closest integer value.

$\sqrt{s}$ (GeV)	88	89	90	91	92	93	94	130	136
L (pb^{-1})	0.7	17.9	0.8	124.8	0.8	19.1	0.8	6.2	6.4
$\sqrt{s}$ (GeV)	161	170	172	183	189	192	196	200	202
L (pb^{-1})	11.1	1.1	9.5	59.2	177.1	28.9	79.8	86.3	42.0

2 The ALEPH detector

The ALEPH detector and its performance are described in Refs. [5, 6]. The tracking detectors, composed of the silicon vertex detector surrounded by the inner tracking chamber and the time projection chamber (TPC), provide efficient reconstruction of charged particles in the angular range $|\cos\theta| < 0.96$. A charged particle track is called a *good track* if it is reconstructed with a least four hits in the TPC and if it originated from within a cylinder of length 20 cm and radius 2 cm, coaxial with the beam and centred at the interaction point. A 1.5 T axial magnetic field delivered by a super-conducting solenoidal coil allows a charged particle $1/\mathrm{p}_\perp$ resolution of $(6 \times 10^{-4} \bigoplus 5 \times 10^{-3}/\mathrm{p}_\perp)(\mathrm{GeV}/c)^{-1}$ to be achieved.

The electromagnetic calorimeter (ECAL) is a lead/wire-plane sampling calorimeter covering the angular range $|\cos\theta| < 0.98$. Anode wire signals provide a measurement of the arrival time of the particles relative to the beam crossing with a resolution better than 15 ns. Cathode pads associated with each wire layer are connected to form projective towers of approximately 0.9° by 0.9° which are read out in three segments in depth. The impact parameter of the photon with respect to the interaction point is estimated from the barycentre of the electromagnetic shower in each segment with a resolution of about 6 cm. A photon candidate is identified using a topological search [6] for energy deposits in neighbouring electromagnetic calorimeter towers isolated from the extrapolation of any charged particle track to the ECAL. Any photon candidate close to a boundary between ECAL modules or pointing towards an uninstrumented region of the TPC is not considered in the analysis. The energy calibration of the ECAL is obtained from Bhabha events, radiative returns to the Z resonance, $\mathrm{e^+e^-} \to \gamma\gamma$ and $\gamma\gamma \to \mathrm{e^+e^-}$ events. The energy resolution for photons is $\delta\mathrm{E/E} = 0.25/\sqrt{\mathrm{E/GeV}} + 0.009$ [6].

The luminosity monitors (LCAL and SICAL) extend the calorimetric coverage down to small polar angles. The iron return yoke is instrumented with streamer tubes and acts as a hadron calorimeter (HCAL), covering polar angles down to 110 mrad. Surrounding the HCAL are two additional double layers of streamer tubes called muon chambers.

The measurements of the tracking detectors and the calorimeters are combined into objects classified as charged particles, photons and neutral hadrons using the energy flow algorithm described in Ref. [6]. All objects are used to compute the total visible energy $\mathrm{E_{vis}}$ and the missing energy $\mathrm{E_{miss}}$ with a resolution of $(0.6\sqrt{\mathrm{E_{vis}/GeV}} + 0.6)$ GeV.

Electron identification is based on the matching between the measured momentum in the tracking system and the energy in the ECAL, the shower profile in the ECAL and the measurement of the specific ionisation energy loss in the TPC. Muons are identified by their characteristic hit patterns in the HCAL and in the muon chambers.

3 Event preselection

Signal events are characterized by two isolated, energetic photons, well contained in the apparatus, and in time with the beam crossing.

Photon isolation is ensured by requiring that the total charged energy in a cone of half-angle 14° around the photon direction ($E^{\gamma}_{14^\circ}$) be smaller than 2 GeV, and that the invariant mass between the photon and any charged particle ($m_{\gamma,\mathrm{ch}}$) be in excess of $1\,\mathrm{GeV}/c^2$. Pairs of photons from a π^0 decay are rejected by the requirement that their invariant mass be larger than $1\,\mathrm{GeV}/c^2$.

Photon centrality is enforced by requiring that the polar angles satisfy $|\cos\theta_\gamma| < 0.9$. Since the Higgs boson is expected to be produced with a nearly uniform $\cos\theta$ distribution, the sum of the two cosines (in absolute value) must be smaller than 1.4, and the cosines of the Higgs boson production and the thrust axis polar angles, $\theta_{\gamma\gamma}$ and θ_{thrust} must be within ± 0.95. Events with energy at low polar angles are further vetoed by rejecting events with more than 2 GeV within 14° of the beam axis ($E^{\mathrm{beam}}_{14^\circ}$).

If, in a selected event, more than two photons satisfy the above criteria, only the most energetic two photons are considered as originating from a Higgs boson candidate.

Finally, only events in time with the beam crossing are kept. For events with at least two good tracks, a timing to better than 1 ns is ensured by the good track definition. Events with only one good track are rejected. The production time of events with no good tracks is determined as the energy-weighted average of the times reconstructed in all ECAL modules, t_0, and is required to be in agreement with the beam crossing time within ± 40 ns. For these events, the impact parameter of each identified photon is also required to be less than 25 cm.

The reconstructed particles of events with at least two good tracks are then forced to form four "jets" with the Durham jet clustering algorithm [7]. The consistency of these events with a four-body final-state hypothesis is verified by requiring that each of the four jet energies E^{resc}_i, rescaled to satisfy energy-momentum conservation under the assumption that the jet velocities are perfectly measured, be positive. However, in order to make the reconstructed Higgs boson mass resolution independent of the final state topology, the measured photon energies were used instead of the rescaled energies.

In the following, the *neutral electromagnetic energy* in a given jet is computed with all neutral objects in the electromagnetic calorimeter, and with the objects in the hadron calorimeter found behind uninstrumented regions of the electromagnetic calorimeter. An *electromagnetic jet* is defined as a jet with more than 80% of electromagnetic energy. In events reconstructed with four jets, *i.e.*, with at least two good tracks, the two jets with the smallest electromagnetic energy fraction are called *fermionic jets*.

At this level, a signal efficiency of 20 to 65% is achieved at all centre-of-mass energies and for any Higgs boson mass above $1\,\mathrm{GeV}/c^2$, as estimated with many $\mathrm{e^+e^-} \to \mathrm{Hf\bar{f}}$ simulated event samples produced with the `HZHA` generator [8] and processed through the whole detector simulation and event reconstruction chain.

4 Event selection

Events passing the above preselection are further classified in the four signal topologies according to their good track multiplicity (n_{ch}).

- Events with no good tracks are classified as $H\nu\bar{\nu}$ candidate events. The main standard model background sources to this final state are *(i)* $e^+e^- \to \nu\bar{\nu}\gamma(\gamma)$, simulated with the KORALZ package [9]; and *(ii)* $e^+e^- \to \gamma\gamma(\gamma)$, simulated with the GGG generator [10]. The latter generator does not contain QED contributions of order α^4 and above, but they were estimated in Ref. [11] to be small enough to be considered negligible in the present analysis.

- Events with two good tracks, both positively identified as electrons or muons, are classified as $H\ell^+\ell^-$ (with ℓ = e or μ) candidate events. The programs BHWIDE [12] and UNIBAB [13] on the one hand, and KORALZ on the other, are employed to simulate the main background processes, *i.e.*, $e^+e^- \to e^+e^-\gamma(\gamma)$ and $\mu^+\mu^-\gamma(\gamma)$, respectively.

- Other two good track events, and events with up to four good tracks are classified as $H\tau^+\tau^-$ candidate events. Here again, the main background process, $e^+e^- \to \tau^+\tau^-\gamma(\gamma)$ is simulated with KORALZ.

- Finally, events with at least five good tracks are classified as $Hq\bar{q}$ candidate events. The $e^+e^- \to q\bar{q}(\gamma)$ process is simulated with JETSET [14] for data taken at the Z resonance, and with PYTHIA [15] and HERWIG [16] at higher energies. The four-fermion processes WW, ZZ, Zee and Weν are simulated using PYTHIA [15].

The selection criteria designed to reduce the contribution of the background processes are summarized in Table 2, and only a brief account is given here.

For each of the topologies, the photons of the $e^+e^- \to f\bar{f}\gamma(\gamma)$ background process are emitted by the incoming and the outgoing charged fermions. They are therefore preferentially produced either along the beam axis or along one of the outgoing charged fermion directions. An efficient rejection is achieved by tightening the photon isolation requirements with respect to these directions, by means of the variables introduced in Section 3 and a number of other relevant variables: *(i)* photon energies E_γ and the energy recoiling against the photon pair E_H^{recoil}, *(ii)* invariant masses ($m_{\gamma,ch}$, $m_{\gamma,f}$) and transverse momentum $p^{\gamma}_{\perp_{ch}}$ of individual charged particles and fermionic jets with respect to the photons, *(iii)* transverse momentum of the photon with respect to the closest fermionic jet $p^{f}_{\perp_\gamma}$ and transverse momentum of the fermionic jets with respect to the thrust axis $p^{thrust}_{\perp_f}$, *(iv)* the value y_{34} of the Durham y_{cut} transition value between three and four jets and the invariant mass of the two fermionic jets $m_{f\bar{f}}$. For the Z peak data, exactly two electomagnetic jets N^{elec}_{jets} are required in order to reject events in which both photons are inside the same jet.

Further cuts are made on the cosine of the decay angle of the photons (fermions) in the rest frame of the $\gamma\gamma$ ($f\bar{f}$) system $\cos\theta^{dcy}_{\gamma\gamma}$ ($\cos\theta^{dcy}_{f\bar{f}}$). These decay angles are expected to have a flat distribution for signal events, while they are strongly peaked towards small angles for

Table 2: Overview of all selection cuts

<table>
<tr><th>Z peak</th><th>High energy</th></tr>
<tr><td>$E_{\gamma_i} > 3\,\mathrm{GeV};\ E_{\gamma}^{\max} > 0.1\sqrt{s}$
$E_{H}^{\mathrm{recoil}} > 10\,\mathrm{GeV};\ E_{\mathrm{visible}} > 0.6\sqrt{s}$</td><td>$0.2E_{\mathrm{beam}} < E_{\gamma_i} < 0.75E_{\mathrm{beam}}$
$|m_{\mathrm{rec}} - m_{Z}| < 15\,\mathrm{GeV}/c^2$</td></tr>
<tr><td colspan="2">No good track: $H\nu\bar{\nu}$</td></tr>
<tr><td colspan="2">$|\cos\theta_{\gamma\gamma}| < 0.9$
$E_{\mathrm{miss}} > 15\,\mathrm{GeV}$
$E_{\mathrm{vis}} - E_{\gamma\gamma} < 10\,\mathrm{GeV}$
$|m_{\gamma\gamma} + m_{\mathrm{rec}} - \sqrt{s}| > 2\,\mathrm{GeV}/c^2$
$|\cos\theta_{\gamma\gamma}^{\mathrm{dcy}}| < 0.95$
$E_{\gamma}^{\max} > 0.15\sqrt{s}$</td></tr>
<tr><td colspan="2">Two good tracks: $H\ell^+\ell^-/H\tau^+\tau^-$</td></tr>
<tr><td colspan="2">$E_i^{\mathrm{resc}} > 0\,\mathrm{GeV}$
$m_{f\bar{f}} > 1\,\mathrm{GeV}/c^2$
$m_{\gamma,\mathrm{ch}} > 5\,\mathrm{GeV}/c^2$
$p_{\perp_{\mathrm{ch}}}^{\gamma} > 2\,\mathrm{GeV}/c$
$m_{\gamma,\mathrm{f}} > 10\,\mathrm{GeV}/c^2$
$p_{\perp_{\mathrm{ch}}}^{\gamma} > 10\,\mathrm{GeV}/c$</td></tr>
<tr><td>$e^+e^-/\mu^+\mu^- : H\ell^+\ell^-$</td><td>$e\mu/eh/\mu h/hh : H\tau^+\tau^-$</td></tr>
<tr><td>$E_{\gamma} > 10\,\mathrm{GeV}$
$|\cos\theta_{\ell^+\ell^-}^{\mathrm{dcy}}| < 0.95$</td><td>$E_{\gamma} > 20\,\mathrm{GeV}$
$|m_{\mathrm{rec}} - m_{f\bar{f}}^{\mathrm{resc}}| < 20\,\mathrm{GeV}/c^2$</td></tr>
<tr><td colspan="2">Three or four good tracks: $H\tau^+\tau^-$</td></tr>
<tr><td colspan="2">$E_i^{\mathrm{resc}} > 0\,\mathrm{GeV}$
$p_{\perp_{\mathrm{f}}}^{\mathrm{thrust}} > 2\,\mathrm{GeV}/c; m_{\gamma,\mathrm{f}} > 10\,\mathrm{GeV}/c^2$
$N_{\mathrm{jets}}^{\mathrm{elec}} = 2;\ E_{\mathrm{miss}} < 15\,\mathrm{GeV}$
$|\cos\theta_{\gamma\gamma}^{\mathrm{dcy}}| < 0.95;\ |\cos\theta_{f\bar{f}}^{\mathrm{dcy}}| < 0.95$
$p_{\perp_{\mathrm{f}}}^{\mathrm{thrust}} > 4\,\mathrm{GeV}/c$</td></tr>
<tr><td colspan="2">Five or more good tracks: $Hq\bar{q}$</td></tr>
<tr><td colspan="2">$E_i^{\mathrm{resc}} > 0\,\mathrm{GeV}$
$|\cos\theta_{\gamma}| < 0.8$
$y_{34} > 0.001$
$p_{\perp_{\mathrm{f}}}^{\mathrm{thrust}} > 2\,\mathrm{GeV}/c; m_{\gamma,\mathrm{f}} > 10\,\mathrm{GeV}/c^2$
$N_{\mathrm{jets}}^{\mathrm{elec}} = 2;\ E_{\mathrm{miss}} < 15\,\mathrm{GeV}$
$|\cos\theta_{\gamma\gamma}^{\mathrm{dcy}}| < 0.95;\ |\cos\theta_{f\bar{f}}^{\mathrm{dcy}}| < 0.95$
$p_{\perp_{\mathrm{f}}}^{\mathrm{thrust}} > 4\,\mathrm{GeV}/c$
$p_{\perp_{\gamma}}^{\mathrm{f}} > 0.05\sqrt{s}$
$\theta_{4-\mathrm{jets}}^{\min} > 350^{\circ}$</td></tr>
</table>

the background. For a high mass Higgs at high energies the signal events are expected to be somewhat spherical in nature. Non-spherical events are rejected by a cut on the sum of the four minimum inter-jet angles $\theta_{4-\mathrm{jets}}^{\min}$. At high energies the mass recoiling against the photonic system m_{rec} is required to be consistent with the Z mass. For the $H\tau\tau$ channel at Z peak energies the mass recoiling against the photonic system is required to be consistent with the rescaled mass of the fermionic system $m_{f\bar{f}}^{\mathrm{resc}}$. Finally, in the $H\nu\bar{\nu}$ topology, some boost is ensured by requiring that the total produced mass does not saturate the available energy: $|m_{\gamma\gamma} + m_{\mathrm{rec}} - \sqrt{s}| > 2\,\mathrm{GeV}$.

The typical efficiencies and expected standard model background for each topology, together with cross-channel contamination, are shown in Table 3.

Table 3: Efficiencies for the different Z decay channels for a 110 GeV/c^2 Higgs boson mass at $\sqrt{s} = 202$ GeV and numbers of expected background and observed events at the Z peak (Z) and at high energies (HE).

n_{ch}	$\epsilon_{H\nu\bar{\nu}}$	$\epsilon_{H\ell^+\ell^-}$	$\epsilon_{H\tau^+\tau^-}$	$\epsilon_{Hq\bar{q}}$	$N_{exp.}^{back.}(Z)$	$N_{obs.}(Z)$	$N_{exp.}^{back.}(HE)$	$N_{obs.}(HE)$
0	47.0%	0.3%	0.0	0.0	0.9	1	3.6	0
2	0.0	36.7%	22.4%	0.0	2.3	4	2.9	2
3-4	0.0	2.0%	14.9%	0.0	0.7	0	0.4	2
$\geq$5	0.0	0.0	5.2%	37.3%	9.3	7	7.8	6
Total	47.0%	39.0%	42.5%	37.3%	13.2	12	14.7	10

5 Systematic uncertainties

Because no background subtraction is performed to derive the final result, the uncertainty on the background evaluation has not been estimated. The uncertainty on the photon selection efficiency summarized in Table 4 receives a large contribution from the photon identification efficiency. The uncertainties due to photon energy calibration or photon angle resolution affect only the $\gamma\gamma$ invariant mass resolution.

To estimate the uncertainty on the photon selection efficiency, the total cross section of the $e^+e^- \to \gamma\gamma(\gamma)$ process was measured and compared to its prediction. Two-photon-candidate events are selected as final states with only two identified photons (with the same timing and pointing constraints as those defined in section 3) with a polar angle such that $|\cos\theta_\gamma| < 0.9$ (0.95), and an opening angle satisfying $\cos\alpha_{\gamma\gamma} < -0.999$ (-0.9999), for the Z peak data (at high energy). The $e^+e^- \to e^+e^-\gamma\gamma$ background is rejected by requiring no charged particles in the event and not more than 2 GeV of energy around the beam direction ($E_{14^\circ}^{beam} < 2$ GeV). The $\nu\bar{\nu}\gamma\gamma$ background is reduced to a negligible amount by requiring the invariant mass of the two-photon system to be greater than $0.75\sqrt{s}$. The result is displayed in Fig. 1. From this measurement, a conservative relative systematic uncertainty is estimated to be 3%, including a 1% theoretical error. The systematic uncertainty on the photon detection efficiency includes the effects of the cuts on photons used at preselection level as well as that of the integrated luminosity determination, which enters the $e^+e^- \to \gamma\gamma(\gamma)$ cross section measurement.

The effect of the photon energy calibration and angular resolution on the efficiency is estimated with Bhabha events. The relative difference between the values of the electron energy determined independently by the tracking system and by the calorimetry mainly originates from electron Bremsstrahlung. This difference is measured to be $\sim 1.5\%$, and it agrees within 0.2% with that expected from the simulation. This $\pm 0.2\%$ uncertainty is conservatively assigned to the photon energy calibration. It leads to a shift of the measured Higgs boson mass by ± 200 MeV/c^2, and to a negligible increase of the mass resolution. The uncertainty on the reconstructed photon direction is estimated by comparing the directions determined with the tracking and the calorimetry. It degrades the measured Higgs boson mass resolution by approximately 20 MeV/c^2 with a negligible loss of efficiency. These systematic uncertainties are included in the final result by increasing the Higgs boson mass resolution by 200 MeV/c^2 .

As the lepton identification is used only to classify events, the signal efficiency decreases by less than 0.1% relative when the lepton identification efficiency is modified by 10%.

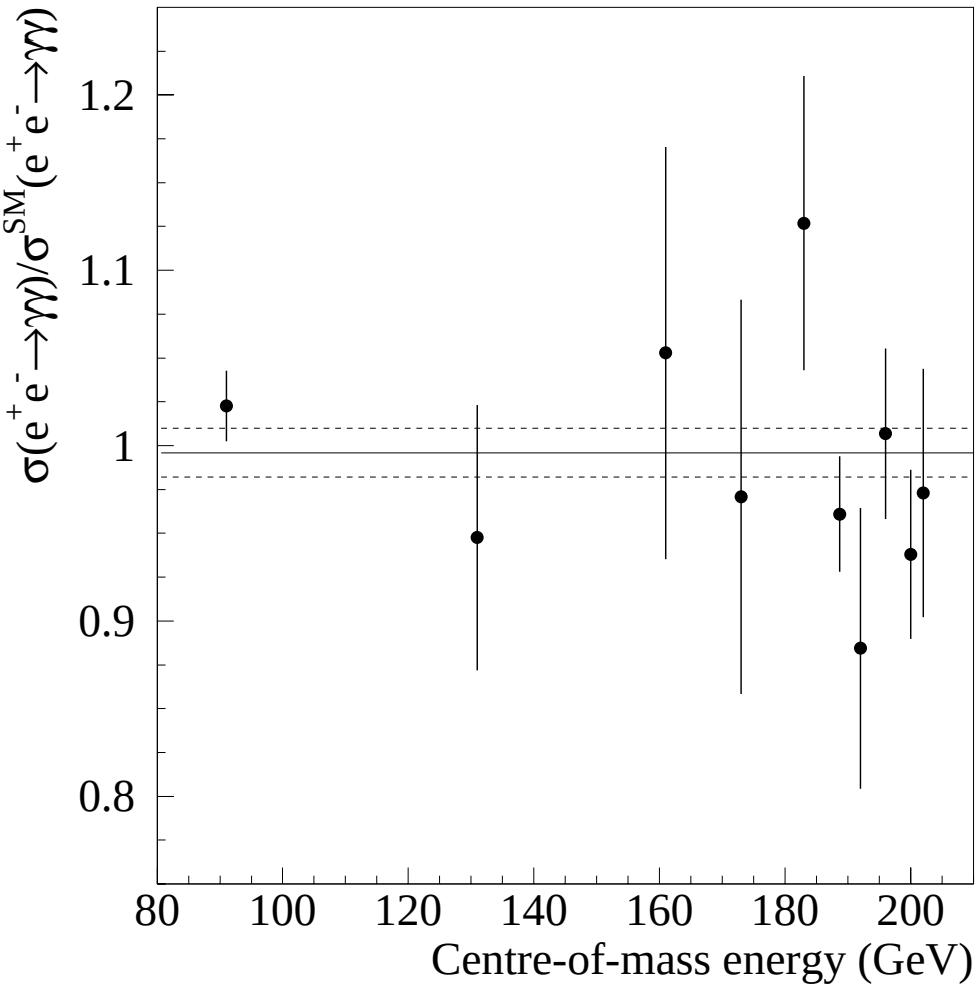

Figure 1: Ratio of the measured cross section of the $e^+e^- \to \gamma\gamma(\gamma)$ process at all centre-of-mass energies to the expected standard model cross section. The solid line is the best fit to the data and the two dotted lines represent the statistical error from the fit.

The remaining selection criteria are expected to be largely insensitive to the details of the simulation of the hadronic system. A quantitative estimate of the size of possible discrepancies is performed with the aid of an event reweighting technique. For each selection variable, bin-by-bin correction factors are calculated as the ratio of data to Monte Carlo expectation, evaluated at the preselection level with the cut on $m_{\gamma,ch}$ removed. The Monte Carlo signal distribution of the selection variable, obtained when all cuts are applied, is then re-weighted with these correction factors to obtain a new estimate of the efficiency. The difference in efficiencies estimated with this technique are, for almost all variables, at the level of a few parts per mil and are given in Table 4. The largest effect, of 1.2%, comes from the cut on the isolation of the photon $m_{\gamma,ch}$.

Finally, the model dependence of this analysis is estimated with the anomalous coupling model mentioned in Section 1. In that context, all the anomalous coupling parameters f_i/Λ^2 are

Table 4: Systematic uncertainties on signal efficiency

Sources	Relative uncertainty in %
Photon selection efficiency	3.0
γ energy calibration	0.5
γ angular resolution	0.1
Total energy calibration (Z peak data only)	0.5
Lepton identification	0.1
Photon isolation	1.2
$\cos\theta_{\mathrm{thrust}}$	0.1
$\mathrm{p}_{\perp_{\mathrm{f}}}^{\mathrm{thrust}}$	0.2
$\mathrm{m}_{\gamma,\mathrm{f}}$	0.3
$\mathrm{p}_{\perp_\gamma}^{\mathrm{f}}$ (High energy data only)	0.4
y_{34}	0.5
$\theta_{4-\mathrm{jets}}^{\mathrm{min}}$ (High energy data only)	0.3
Model dependence	4.0
Total in quadrature	5.2

varied independently of each other within ± 100 TeV^{-2} using the HZHA generator. The influence of the Higgs boson energy and angular distributions leads to a relative uncertainty on the signal efficiency of at most 4%.

The decay width of the Higgs boson is in general negligible with respect to the detector resolution (below 1 GeV for $|\mathrm{f}_i/\Lambda^2| < 100$ TeV^{-2}). In anomalous coupling models with $|\mathrm{f}_i/\Lambda^2|$ above 500 TeV^{-2} the decay width of a heavy Higgs boson becomes larger than the detector invariant mass resolution ($\Gamma \approx 3$ GeV) and the relative variation of the signal efficiency becomes larger than the previously estimated systematic uncertainties. The final results presented in the next section are therefore valid for models in which the width of the Higgs boson is less than a few GeV.

6 Results

The signal efficiencies are displayed in Fig. 2a as a function of the Higgs boson mass hypothesis. Twenty-two events are selected in the data compared with an expectation of 27.9 ± 1.6 events from all standard model background processes. The contributions of the various channels are given in Table 3. The diphoton invariant mass distribution of these selected events is shown for both data and Monte Carlo expectation in Fig. 2b. The low mass background is dominated by events where both photons originated from the same jet, whereas the high mass background is dominated by events where the two photons originated from different jets. The sum of these two contributions has a minimum at around $8\,\mathrm{GeV}/c^2$. No evidence of a resonance decaying to $\gamma\gamma$ is observed and a 95% confidence level upper limit on the number of signal events at a given diphoton invariant mass is derived following the method described in Ref. [17]. For each LEP energy, the total efficiency and the mass resolution are parametrized as a function of the $\gamma\gamma$ invariant mass. The diphoton invariant mass resolution varies linearly from 1 GeV/c^2

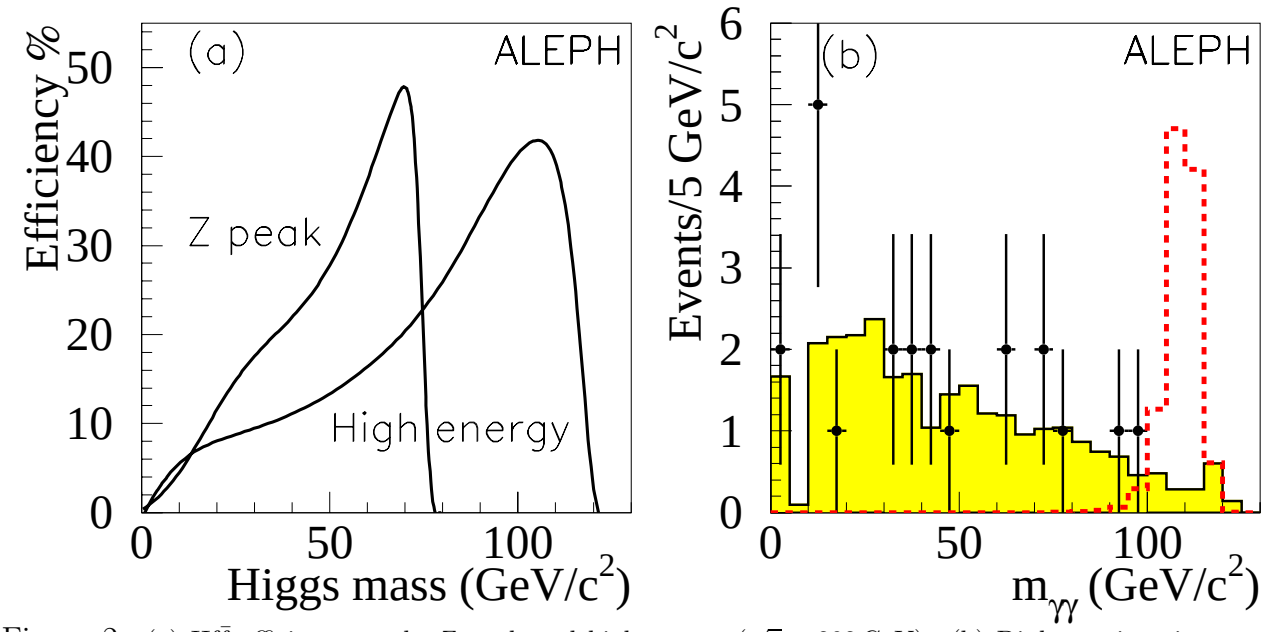

Figure 2: (a) $\mathrm{Hf\bar{f}}$ efficiency at the Z peak and high energy ($\sqrt{s} = 202\,\mathrm{GeV}$). (b) Diphoton invariant mass distribution for data (dots with error bar), expected sources of background (solid histogram) and a $110\,\mathrm{GeV}/c^2$ Higgs boson signal at $\sqrt{s} = 202\,\mathrm{GeV}$ with arbitrary normalization (dashed histogram).

to 3.5 GeV/c^2 over the whole Higgs boson mass range. The systematic uncertainties are conservatively taken into account by scaling down the efficiency by 5.2% and increasing the mass resolution as described in the previous section.

The present analysis does not apply for Higgs boson masses below 1 GeV/c^2. To extend the search to smaller masses, the direct measurement of the Z invisible width with single photon counting described in Ref. [18] was used. For this measurement, the single photon candidate events were selected as final states with only one cluster in the electromagnetic calorimeter. The $\mathrm{H}\nu\bar{\nu}$ events with $\mathrm{m_H} < 1\,\mathrm{GeV}/c^2$ would therefore have been selected with a good efficiency, ranging from 13 to 45%, thus leading to a sensitivity similar to that of the present analysis.

Assuming a Higgs boson production cross section with the same $\sqrt{s}, \mathrm{m_H}$ dependencies as in the standard model, the 95% confidence level upper limit on the product branching ratio $\mathrm{B(H} \to \gamma\gamma)\sigma(\mathrm{e^+e^-} \to \mathrm{Hf\bar{f}})/\sigma^{\mathrm{SM}}(\mathrm{e^+e^-} \to \mathrm{Hf\bar{f}})$ is derived and shown in Fig. 3.

For the case of a Higgs boson produced at the standard model rate, the best upper limit on the branching ratio ($4.7{\times}10^{-3}$ at 95% confidence level) is obtained for Higgs boson masses below 20 GeV/c^2. A Higgs boson decaying exclusively to two photons is ruled out up to 109 GeV/c^2 at 95% confidence level.

A fermiophobic Higgs boson [19] with no tree-level coupling to fermions is excluded at 95% confidence level for any mass up to 100.7 GeV/c^2.

The present analysis extends the reach of similar analyses performed by other LEP collaborations [20–22].

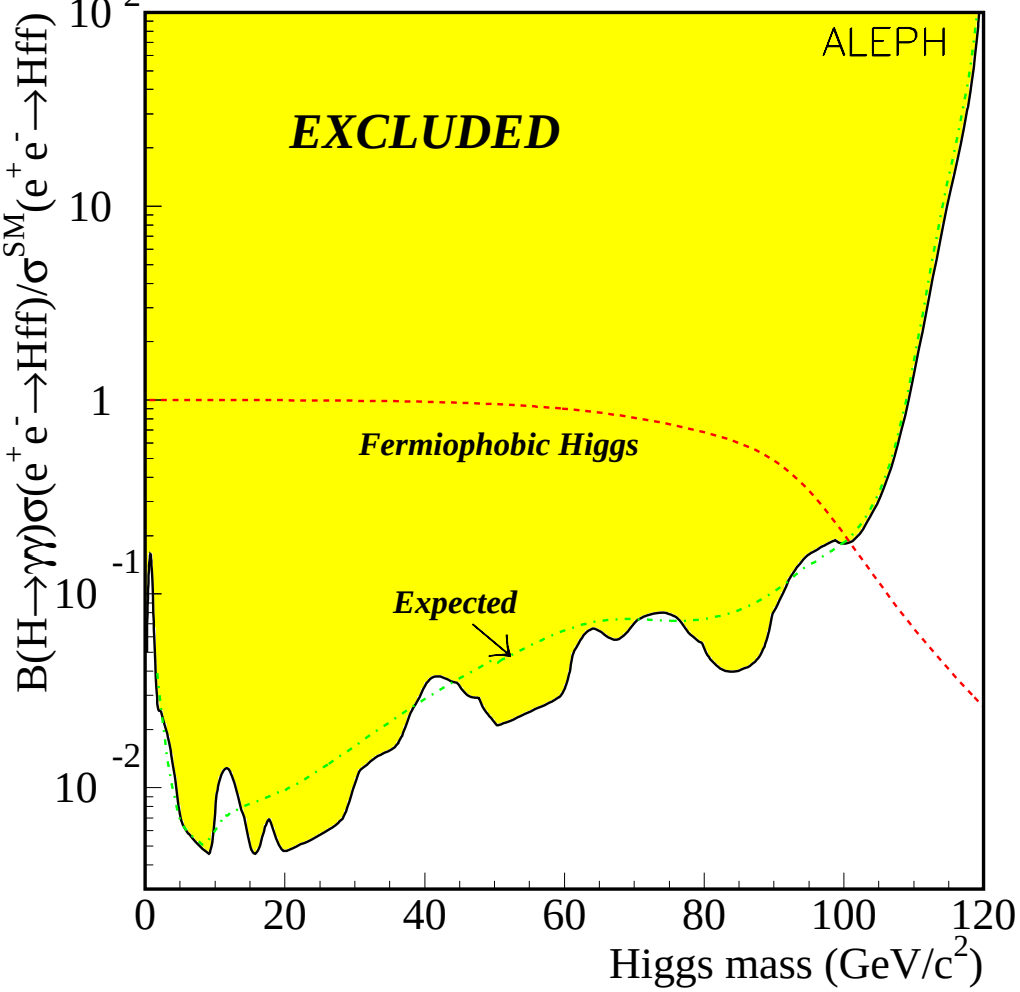

Figure 3: Measured (full curve) and expected (dash-dotted curve) 95% confidence level upper limit on $B(H \to \gamma\gamma)\sigma(e^+e^- \to Hf\bar{f})/\sigma^{SM}(e^+e^- \to Hf\bar{f})$. The dashed curve is the predicted branching ratio for a fermiophobic Higgs boson in the limit of $B(H \to f\bar{f}) = 0$.

7 Conclusion

With a data sample of 672 pb^{-1} recorded at centre-of-mass energies from 88 GeV to 202 GeV, a search for two photon decays of Higgs bosons produced in association with a fermion pair has been performed in the mass range from 0 up to 120 GeV/c^2. No evidence for resonant production of photon pairs has been found. In the framework of Higgs bosons with standard model coupling to gauge bosons, a 95% confidence level upper limit on the Higgs boson branching ratio to two photons has been obtained for Higgs boson masses from 0 to 109 GeV/c^2. In the fermiophobic model in which the Higgs boson couples exclusively to gauge bosons, a 95% confidence level lower limit on the Higgs boson mass has been set at 100.7 GeV/c^2.

8 Acknowledgements

We wish to thank our colleagues from the CERN accelerator divisions for the successful operation of LEP. We are indebted to the engineers and technicians in all our institutions for their contribution to the excellent performance of ALEPH. Those of us from non-member countries thank CERN for its hospitality.

References

[1] J. Ellis, M. K. Gaillard and D.V. Nanopoulos, *"A Phenomenological Profile of the Higgs Boson"*, Nucl. Phys. **B106** (1976) 292;
A. Djouadi, J. Kalinowski and M. Spira, *"*`HDECAY`*: A Program for Higgs Boson Decays in the Standard Model and its Supersymmetric Extention"*, Comput. Phys. Commun. **108** (1998) 56.

[2] A. G. Akeroyd, *"Fermiophobic Higgs Bosons at the Tevatron."*, Phys. Lett. **B368** (1996) 89;
H. Haber, G. Kane and T. Sterling, *"The Fermion Mass Scale and Possible Effects of Higgs Bosons on Experimental Observables"*, Nucl. Phys. **B161** (1979) 493.

[3] K. Hagiwara, R. Szalapki and D. Zeppenfeld, *"Anomalous Higgs Boson Production and Decay"*, Phys. Lett. **B318** (1993) 155.

[4] ALEPH Collaboration, *"Search for neutral Higgs bosons of the Standard Model and the MSSM in* e^+e^- *collisions at* $\sqrt{s} = 189\,\mathrm{GeV}$*"*, CERN-EP/2000-019, submitted to Eur. Phys. J. C.

[5] ALEPH Collaboration, *"ALEPH: A detector for Electron-Positron Annihilations at LEP"*, Nucl. Instrum. and Methods **A294** (1990) 121.

[6] ALEPH Collaboration, *"Performance of the ALEPH Detector at LEP"*, Nucl. Instrum. and Methods **A360** (1995) 481.

[7] W.J Stirling, *"Hard QCD Working Group: Theory Summary"*, J. Phys. **G17** (1991) 1567.

[8] P. Janot, *"The* `HZHA` *generator"* in *"Physics at LEP 2."*, edited by G.Altarelli. For recent updates, see also: http://alephwww.cern.ch/~janot/Generators.html.

[9] S. Jadach et al., *"The Monte Carlo program* `KORALZ`*, version 3.8, for the lepton or quark pair production at LEP / SLC energies"*, Comput. Phys. Commun. **66** (1991) 276.

[10] F. A. Berends and R. Kleiss, *"Distributions For Electron - Positron Annihilation Into Two And Three Photons"*, Nucl. Phys. **B186** (1981) 22.

[11] ALEPH Collaboration, *"Single- and multi-photon production in* e^+e^- *collisions at a centre-of-mass energy of 183 GeV"*, Phys. Lett. **B429** (1998) 201.

[12] S. Jadach, W. Placzek and B. F. L. Ward, *"BHWIDE 1.00: $O(\alpha)$ YFS exponentiated Monte Carlo for Bhabha scattering at wide angles for LEP1/SLC and LEP2"*, Phys. Lett. **B390** (1997) 298.

[13] H. Anlauf et al., *"UNIBAB, version 2.0: Monte Carlo event generation for large angle Bhabha scattering at LEP"*, Comput. Phys. Commun. **79** (1994) 466.

[14] T. Sjöstrand, *"The LUND Monte Carlo for* e^+e^- *jet physics"*, Comput. Phys. Commun. **28** (1983) 229.

[15] T. Sjöstrand, *"High-energy physics event generation with PYTHIA 5.7 and JETSET 7.4"*, Comput. Phys. Commun. **82** (1994) 74.

[16] G. Marchesini et al., *"HERWIG: A Monte Carlo event generator for simulating hadron emission reactions with interfering gluons. Version 5.1"*, Comput. Phys. Commun. **67** (1992) 465.

[17] P. Janot, F. Le Diberder, *"Optimally combined confidence limits"* , Nucl. Instrum. and Methods **A411** (1998) 449;
ALEPH Collaboration, *"Search for the standard model Higgs boson in* e^+e^- *collisions at* $\sqrt{s}$ *= 161 GeV, 170 GeV and 172 GeV"*, Phys. Lett. **B412** (1997) 155.

[18] ALEPH Collaboration, *"A Direct measurement of the invisible width of the Z from single photon counting"*, Phys. Lett. **B313** (1993) 520.

[19] A. Stange, W. Marciano, and S. Willenbrock, *"Higgs bosons at the Fermilab Tevatron"*, Phys. Rev. **D49** (1994) 1354.

[20] DELPHI Collaboration, *"Search for the Higgs boson in events with isolated photons at LEP 2"*, Phys. Lett. **B458** (1999) 431.

[21] L3 Collaboration, *"Search For New Particles In Hadronic Events With Isolated Photons"*, Phys. Lett. **B 388** (1996) 409.

[22] OPAL Collaboration, *"Search for Higgs Boson and Other Massive States Decaying into Two Photons in* e^+e^- *Collisions at 189 GeV"*, Phys. Lett. **B 464** (1999) 311.